Collective eigenstates of emission in an *N*-entity heterostructure and the evaluation of its Green tensors and self-energy components

Murugesan Venkatapathi

Computational Photonics Laboratory, SERC, Indian Institute of Science, Bangalore 560012, India (murugesh@serc.iisc.ernet.in)

Received July 9, 2014; revised October 30, 2014; accepted October 31, 2014; posted November 4, 2014 (Doc. ID 216706); published November 24, 2014

Optical emission from emitters strongly interacting among themselves and also with other polarizable matter in close proximity has been approximated by emission from independent emitters. This is primarily due to our inability to evaluate the self-energy matrices and radiative properties of the collective eigenstates of emitters in heterogeneous ensembles. A method to evaluate self-energy matrices that is not limited by the geometry and material composition is presented to understand and exploit such collective excitations. Numerical evaluations using this method are used to highlight the significant differences between independent and the collective modes of emission in nanoscale heterostructures. A set of *N* Lorentz emitters and other polarizable entities is used to represent the coupled system of a generalized geometry in a volume integral approach. Closed form relations between the Green tensors of entity pairs in free space and their correspondents in a heterostructure are derived concisely. This is made possible for general geometries because the global matrices consisting of all free-space Green dyads are subject to conservation laws. The self-energy matrix can then be assembled using the evaluated Green tensors of the heterostructure, but a decomposition of its components into their radiative and nonradiative decay contributions is nontrivial. The relations to compute the observables of the eigenstates (such as quantum efficiency, power/energy of emission, radiative and nonradiative decay rates) are presented. A note on extension of this method to collective excitations, which also includes strong interactions with a surface in the near-field, is added.

OCIS codes: (270.1670) Coherent optical effects; (270.6630) Superradiance, superfluorescence; (160.4236) Nanomaterials.

http://dx.doi.org/10.1364/JOSAB.31.003153

1. INTRODUCTION

The interactions of atoms, fluorescing molecules, and quantum dots with metal particles/surfaces have been extensively studied for their effect on the decay rates and radiated power of spontaneous emission [1–8]. But such understanding of the effects of surrounding matter on spontaneous emission has been limited to an independent emitter interacting with a surface [3], particle [4], or a set of spherical particles [8], which are generalized as the Purcell effect. Recently, this was extended by a theoretical study to a set of many emitters interacting collectively with a single spherical metal particle at the center [9,10]. Strongly interacting emitters present collective excitations mediated by virtual photons, and in the presence of other matter can include other virtual excitations as well, for example, plasmons of a metal particle. We should expect that when the interactions between a single emitter and a body are not strong relative to the possible multilateral modes, the collective effects can manifest robustly to be observed and exploited. The impediment in understanding collective heterogeneous systems has been the difficulty of evaluating the self-energy components that include the possible virtual interactions among the emitters. The spontaneous emission from a completely isolated emitter is caused by vacuum fluctuations, while virtual interactions with other proximal matter can change both decay rates and the energy of emission. The effects of such virtual interactions on the spontaneous emission in an emitter-body system or an ensemble of emitters are typically well represented by coupled oscillators that radiate the quantum of energy each [8–10]. In a general heterogeneous ensemble, the evaluation of Green tensors coupling emitters in the presence of all other polarizable matter in proximity becomes necessary in this approach. Special cases of nonclassical emission, where the above method may need modifications, are discussed later.

The diagonal terms of the self-energy matrices of such a heterogeneous system include the independent emitters interacting with other bodies, and these are represented by the self-field of the single emitter due to other polarizable bodies [11]. Whereas the off-diagonal terms of the self-energy matrix include the interactions among any two emitters directly and through other matter in proximity, here we require these Green tensors explicitly. Note that analytical expressions for Green tensors are difficult in general [11], and a numerical evaluation of Green tensors is a preferred approach for complex geometries. Mode decomposition and eigenfunction-based Green-tensor representation is suitable for regular geometries; however, it is seldom a possibility in realistic nanostructures. We start with a set of *n*-Lorentz dipole oscillators, which when coupled can be used to elucidate the conventional Dicke effect of collective emission and the radiative

coupling among them. In addition, here we have m other polarizable entities, which can be sub-volumes of a larger body in a volume integral approach. Thus this method is general and precise for arbitrary shapes, properties, and a number of emitters/bodies, even in the limits where long wavelength approximations are not valid. It is shown that a problem posed by dipole sources and null field conditions at polarizable volumes can be used to evaluate the modified Green tensors coupling the n emitters in presence of the m other polarizable entities. We use matrix algebra to derive closed-form relations between these modified Green tensors and the set of Green dyads coupling pairs of the N (where $N = n + m$) entities in free space (or a homogeneous background). The free-space Green dyads of dipolar entities can be trivially derived by the dyadic operations on scalar Green functions of point dipoles. Use of free space dyads of multipoles to avoid a fine discretization of a body into dipoles is also possible for very large problems. The modified Green tensors coupling the emitters are then used to assemble their self-energy matrix and evaluate their eigenstates. Determining the characteristics of emission from the ensemble involves the additional exercise of decomposing the imaginary part of the self-energy matrices into their radiative and nonradiative parts. This allows us to evaluate the quantum efficiency, decay rates, and the radiated energy/power in the ensemble given the quantum efficiency and nonradiative relaxation of an isolated emitter. The microscopic aspects in dipole representations of certain types of emitters [12,13] and an explicit quantization of the emitter/bodies [14–17] are not the subject of this work, and these may be introduced in this method without loss of generality for any special cases.

Finally, we conclude with a few numerical results highlighting that self-energy matrices of such interacting systems can reveal collective effects hitherto unexplained. Some of our recent experimental observations and their analysis will be described elsewhere. Additions to this method that can include strong interactions of all the N entities with a surface are presented in Appendix B.

2. METHODS

Consider the excitations in independent emitters as oscillating dipole moments with a resonant frequency ω_o. It is assumed that nonradiative relaxations at a decay rate Γ_o^{nr} and uncorrelated emission events at a decay rate Γ_o^r occur in these individual emitters, and they are much slower than the oscillations, i.e., $\Gamma_o^r \ll \omega_o$, and we use classical Lorentz oscillators to represent the excitations. This section has three parts. First self-energy matrices of a collection of coupled Lorentz oscillators and their significance in studying collective behavior in an emission process are discussed. Then this approach is extended to the evaluation of the self-energy matrices for cases where the emitters also interact strongly with other matter. This primarily involves evaluating the Green tensors coupling the emitters in the presence of other polarizable matter in a generalized geometry. Finally we proceed to a technique to decompose the radiative and nonradiative contributions to each self-energy component of the self-energy matrix representing a heterogeneous mixture of emitters with other polarizable bodies. This is essential because the radiative and nonradiative decay matrices determine the observables and measurements of the collective emission.

A. Self-Energy Matrix of Coupled Lorentz Oscillators

The emission from n dipole oscillators interacting with each other is well represented by a coupled system with n eigenstates, some of which are super radiant, and this collective phenomenon of emitters interacting directly is known as the conventional Dicke effect [18–21]. The mechanical force of an oscillating dipole moment, $P_j(t)$, and the force of driving fields from the other Lorentz dipoles, $F_{jk}(t)$, have to be balanced. This results in Eq. (1), where derivatives with respect to time t are represented by the corresponding number of dots in the superscript:

$$[\ddot{P}_j(t) + \Gamma_o^r \dot{P}_j(t) + \omega_o^2 P_j(t)] - \frac{q}{m}\sum_{k\neq j} F_{jk}(t) = 0. \tag{1}$$

Let $P_j\mathbf{e}_j$ be the known dipole moment amplitudes of the interacting Lorentz oscillators with unknown cooperative phases ϕ_j, and let q, m be the magnitude and mass of the charge in the dipoles. We derive the shifts in energy Δ and the modified decay rates Γ of the interacting ensemble due to additional components of self-energy of these emitters immersed in their common field. In the above, the interaction between dipoles can be described in terms of the free-space Green dyads $\mathbf{G}_o$ (a tensor of orientation dependent Green functions), where $(4\pi\omega^2/c^2)\cdot\mathbf{G}_o(\mathbf{r},\mathbf{r}_j;\omega)\cdot\mathbf{e}_j P_j(\omega)e^{i\phi_j} = \mathbf{E}(\mathbf{r},\omega)$, the harmonic component of the electric field at $\mathbf{r}$ due to an isolated dipole moment $P_j\mathbf{e}_j$ at $\mathbf{r}_j$. The above relations for coupled Lorentz oscillators can then be rewritten into the following after factoring out $e^{i\omega t}$:

$$(\omega_o^2 - \omega^2 + i\Gamma_o^r\omega)\cdot P_j(\omega)e^{i\phi_j} - \sum_{k\neq j}\frac{4\pi\omega^2 q^2}{mc^2}\mathbf{e}_j \cdot \mathbf{G}_o(\mathbf{r}_j,\mathbf{r}_k;\omega)\cdot\mathbf{e}_k P_k(\omega)e^{i\phi_k} = 0. \tag{2}$$

For all $\omega \approx \omega_o$, it simplifies to

$$\left(\omega_o - \omega + \frac{i\Gamma_o^r}{2}\right)\cdot P_j(\omega)e^{i\phi_j} - \sum_{k\neq j}\frac{2\pi q^2\omega}{mc^2}\mathbf{e}_j \cdot \mathbf{G}_o(\mathbf{r}_j,\mathbf{r}_k;\omega)\cdot\mathbf{e}_k P_k(\omega)e^{i\phi_k} = 0. \tag{3}$$

Specifically, the Green dyads $\mathbf{G}_o(\mathbf{r}_j,\mathbf{r}_k;\omega)$ of the point dipole oscillators in free space (or a homogeneous medium with permittivity ε) can be derived from the following, where the wave number $k = \sqrt{\varepsilon}\cdot\omega/c$ and c is the speed of light:

$$\nabla\times\nabla\times\mathbf{G}_o(\mathbf{r},\mathbf{r}_j;\omega) - k^2\mathbf{G}_o(\mathbf{r},\mathbf{r}_j;\omega) = \mathbf{I}\delta(\mathbf{r}-\mathbf{r}_j). \tag{4}$$

By substitution of Δ_{jk} and $i\Gamma_{jk}/2$ for the real and imaginary parts of the dipole cross-interaction terms ($j \neq k$) in Eq. (3), we get Eq. (5) after a phase conjugation. The system of equations reduces to a form where the energy shifts and modified decay rates of a dipole due to its interaction with other dipoles can be readily interpreted:

$$\sum_k\left[\left(\omega_o - \omega - \frac{i\Gamma_0^r}{2}\right)\delta_{jk} + \Delta_{jk} - \frac{i\Gamma_{jk}}{2}\right]\cdot P_k(\omega)e^{-i\phi_k} = 0. \tag{5}$$

Let

$$\Sigma_{jk} = \Delta_{jk} - \frac{i\Gamma_{jk}}{2} = \frac{-2\pi q^2 \omega}{mc^2}\mathbf{e}_j \cdot \mathbf{G}_o(\mathbf{r}_j, \mathbf{r}_k; \omega) \cdot \mathbf{e}_k - \delta_{jk}\frac{i\Gamma_0^r}{2} \quad (6)$$

$$\Rightarrow \sum_k \left[(\omega_o - \omega)\delta_{jk} + \Sigma_{jk}\right] \cdot P_k e^{-i\phi_k} = 0. \quad (7)$$

It is convenient to represent the coupled system of equations by the matrix eigenvalue problem in Eq. (7). The unknown cooperative phases ϕ_j for the known oscillating dipole moments P_j are given by the collective eigenstates of the oscillators that are solutions for Eq. (7). These eigenstates are represented by the eigenvalues and eigenvectors of the self-energy matrix Σ. A set of radiating coupled Lorentz oscillators with known starting phases ϕ_j and initial dipole-moment amplitudes P_j are equally well represented by the self-energy matrix in Eq. (6), as shown elsewhere [10]. The real part of its eigenvalues represents the energy shifts of a collective eigenstate, and corresponding decay rates are given by its imaginary part. Thus they represent a system of coupled equations that are fully satisfied by $(-\lambda I + \Sigma)V = 0$, where λ are the eigenvalues and V is the set of eigenvectors representing the eigenstates. Calculation of eigenvalues of $\Sigma(\omega_o)$ may be sufficient in some cases to determine modified decay rates and shifts of emission energies when $\Gamma_o^r \ll \omega_o$. A weighted numerical integration of $\Sigma(\omega)$ is also straightforward (and the diagonal term representing radiative decay of an emitter in a vacuum can be added after this integration). Thus we include the relevant energy spectrum only where the Lorentzian dipole moments $P(\omega)$ are significant, as given in Eq. (9), where P_o is the initial dipole moment. Further, the excitations of dipole oscillators are given the total energy of a quantum of radiation:

$$\Gamma_o^r = \frac{2}{3}\frac{kq^2\omega_o}{mc^2} = \frac{2}{3}\frac{k^3 P_o^2}{\varepsilon_o \hbar} \quad \text{and} \quad \frac{P_o}{q} = \left(\frac{\hbar}{m\omega_o}\right)^{1/2}, \quad (8)$$

where

$$P(\omega) = \frac{P_o}{4\pi}\frac{\Gamma_o^r}{(\omega_o - \omega)^2 + (\Gamma_o^r/2)^2}. \quad (9)$$

The interaction with another emitter results in energy shifts given by the real parts of the off-diagonal terms of the self-energy matrix, and the corresponding change in decay rates are given by the imaginary parts. The diagonal terms of the self-energy matrix represents the case of the independent or the uncoupled emitter and contains only its radiative decay rate. Energy shifts (or a change in resonant frequency to $\omega \neq \omega_o$) appear even for the independent emitter when it interacts with other bodies, as seen in the next section. Energy shifts in the emission can be interpreted as an equivalent shift in the ratio of the electrical self-interaction and mass of the dipole emitters. In the theoretical approach so far, internal nonradiative relaxations of the dipole emitters have not been included, and these can be explicitly added in the diagonal terms of Σ just as the radiative decay rates of the independent emitter [see Eq. (23)]. This involves the assumption that internal nonradiative relaxation of an emitter is independent of its radiative decay. Thus, using a harmonic oscillator to represent the single quantum of emission has been the typical approach. Alternately, the Lorentz oscillators can be assigned an energy that includes both the radiative and nonradiative decay of the emission. This allows for the inclusion of nonradiative interaction of two oscillators in proximity and the total mechanical energy of the oscillator increases by a factor $1/Q_o$ while the radiative decay includes only a quantum of energy as in Eq. (10). Note that in this case Lorentz factors will include the total decay rates Γ_o instead of Γ_o^r used above. The method presented in this paper is amenable to both definitions of the oscillators. The latter are useful in cases where emitters are also coupled nonradiatively and when dipole–dipole interactions are sufficient to model this nonradiative coupling:

$$\Gamma_o^r = \frac{2}{3}\frac{kq^2\omega_o}{mc^2} = \frac{2Q_o k^3 P_o^2}{3\varepsilon_o \hbar} \quad \text{and} \quad \frac{P_o}{q} = \left(\frac{\hbar}{Q_o m\omega_o}\right)^{1/2}, \quad (10)$$

$$\text{and } Q_o = \frac{\Gamma_o^r}{\Gamma_o^r + \Gamma_o^{nr}} \quad \text{and} \quad \Gamma_o^r + \Gamma_o^{nr} = \Gamma_o. \quad (11)$$

Further, the above description of the collective emission process is restricted by only certain cases where the number of excitations participating in the collective emission process is not small compared to the number of optical states at energy $\sim\hbar\omega_o$, which is typically large. This situation is possible inside micro-cavities and photonic crystals when specifically the emission energies are near the edges of a band gap [22], and a strong excitation includes a sufficient density of such emitters in this emission process. Also, a set of emitters can coherently share fewer excitations resulting in emissions of a higher decay rate [23]. Such special cases of nonclassical emission may require a more explicit quantization of the field or the individual components of the self-energy matrix, and fortunately, do not include a wide variety of heterogeneous optical materials and their emission.

B. Evaluation of Green Tensors and Self-Energy Components of a Heterostructure

When emitters are neither in vacuum nor in a homogeneous dielectric medium and interact with other polarizable bodies in proximity, evaluation of the Green tensors coupling them is nontrivial. Using a volume integral approach, a heterogeneous volume can be represented by sub-volumes with corresponding permittivity. In the presence of m other polarizable volumes, much smaller than the wavelength in dimensions, the Green dyads are determined using the following Maxwell's equation for a heterostructure in a homogeneous background medium:

$$\omega^2\varepsilon(\omega)\mathbf{E}(\mathbf{r},\omega) - c^2\nabla\times\nabla\times\mathbf{E}(\mathbf{r},\omega) = -4\pi\omega^2\left\{\sum_{j=1}^{n} P_j(\omega)\mathbf{e}_j\delta(\mathbf{r}-\mathbf{r}_j) + \sum_{j=n+1}^{N=n+m}\bar{\alpha}_j(\omega)\delta(\mathbf{r}-\mathbf{r}_j)\mathbf{E}(\mathbf{r},\omega)\right\}. \quad (12)$$

Here, $\bar{\alpha}_j$ and ε are the polarizability tensor of volume j and the permittivity of the homogeneous background, respectively. An analytical solution of this discrete problem, with or without solving for these modified Green dyads, is an intractable problem in general. But the free-space Green dyads of point dipoles can be derived from Eq. (4) using outgoing spherical scalar waves from a point source in a

homogeneous infinite medium (with permittivity ε) as given below:

$$\mathbf{G}_o(\mathbf{r}_j,\mathbf{r}_k;\omega)=\left[\bar{\mathrm{I}}+\frac{c^2\nabla\nabla}{\omega^2}\right]g(R)$$
$$\text{where } g(R)=(4\pi R)^{-1}\exp\left(i\frac{\omega\sqrt{\varepsilon}}{c}R\right),\quad R=\|\mathbf{r}_j-\mathbf{r}_k\|, \tag{13}$$

when the background medium is isotropic [with permittivity $\varepsilon(\mathbf{r}\neq\mathbf{r}_j)=\varepsilon$].

Using the above, solutions of Eq. (12) can be rewritten into a problem of N oscillators coupled by $\mathbf{G}_o(\mathbf{r}_j,\mathbf{r}_k;\omega)$, the Green dyad in the homogeneous background medium. These are

$$\frac{4\pi\omega^2}{c^2}\bar{G}_o\cdot P=E, \tag{14}$$

where

$$\bar{G}_o=\left[\begin{array}{c|c} \bar{G}_o^{ee}(j,k)=\mathbf{G}_o(\mathbf{r}_j,\mathbf{r}_k;\omega) & \bar{G}_o^{eb}(j,k)=\mathbf{G}_o(\mathbf{r}_j,\mathbf{r}_{n+k};\omega) \\ j,k=1\ldots n & j=1\ldots n,k=1{:}m \\ \text{size:}3n\times3n & \text{size:}3n\times3m \\ \hline \bar{G}_o^{be}(j,k)=\mathbf{G}_o(\mathbf{r}_{n+j},\mathbf{r}_k;\omega) & \bar{G}_o^{bb}(j,k)= \\ j=1\ldots m,k=1\ldots n & \mathbf{G}_o(\mathbf{r}_{n+j},\mathbf{r}_{n+k};\omega)-\delta_{jk}\bar{\alpha}_{n+j}^{-1}(\omega) \\ \text{size:}3m\times3n & j,k=1\ldots m \text{ and size:}3m\times3m \end{array}\right],$$

$$P=\begin{bmatrix} P^e \\ 3n\times1 \\ \hline P^b \\ 3m\times1 \end{bmatrix}=\begin{bmatrix} \mathbf{P}_j^e \\ j=1\ldots n \\ \hline \mathbf{P}_j^b \\ j=n+1\ldots n+m \end{bmatrix},$$

$$E=\begin{bmatrix} E^e \\ 3n\times1 \\ \hline E^b \\ 3m\times1 \end{bmatrix}=\begin{bmatrix} \mathbf{E}_j^e \\ j=1\ldots n \\ \hline \mathbf{0} \\ j=n+1\ldots n+m \end{bmatrix}. \tag{15}$$

Writing such global matrices containing the Green dyads coupling, each pair of entities gives us a concise representation but, more importantly, helps unravel the implicit relations between Green dyads required to satisfy the conservation laws. The global matrix of Green dyads $\bar{G}_o$ can be decomposed further into four parts: $\bar{G}_o^{ee}$, direct interaction between pairs of emitters; $\bar{G}_o^{bb}$, interaction among the pairs of m polarizable bodies; and $\bar{G}_o^{eb},\bar{G}_o^{be}$, representing the interaction between an emitter-body pair, which are transposes of each other (as the individual Green dyads are symmetric). $\bar{G}_o^{bb}$ has its diagonal dyads constituted by $-\bar{\alpha}^{-1}$ while $\bar{G}_o^{ee}$ has zeros in diagonal dyads correspondingly for the self-interaction terms (radiation reaction and nonradiative loss) of the independent emitter. Γ_o can be conveniently included in the self-energy matrices as in Eqs. (22) and (23), which are shown later. The polarizability tensor $\bar{\alpha}$ can be corrected for subvolumes of a contiguous large body using lattice dispersion relations if required [24]. Such finer volume discretization of a body is needed if its dimensions are not much smaller than the wavelength of emission. This limit becomes more stringent if two distinct bodies are closely spaced, for example, when distance between centers $\to 2a$, where a is the radius of a spherical particle. We will revisit multipolar representations of a body later in the paper. Otherwise polarizability of a distinct particle much smaller than the wavelength is well approximated by its dipole polarizability. In case of an isotropic material this reduces to

$$\alpha_j(\omega)=a^3\left[\frac{\varepsilon(\omega,\mathbf{r}_j)-\varepsilon}{\varepsilon(\omega,\mathbf{r}_j)+2\varepsilon}\right], \tag{16}$$

where a is radius of particle.

In the above problem, the polarizations of the m bodies P^b and the collective self-fields at the n emitters E^e are unknown, but these do not have to be explicitly solved for. The required Green dyads can be implicitly derived by rewriting the problem in terms of the required global matrix of green dyads $\bar{G}^{ee}$, coupling pairs of the n emitters in this heterostructure, and resulting in these collective self-fields E^e. This matrix should contain the required sum of the Green dyad in a background homogeneous medium and its perturbation $\mathbf{G}_h(\mathbf{r}_j,\mathbf{r}_k;\omega)$ by the heterostructure, ordered by the block indicated definition in Eq. (15):

$$\frac{4\pi\omega^2}{c^2}\bar{G}^{ee}\cdot P^e=E^e, \tag{17}$$

where $\bar{G}^{ee}(j,k)=\mathbf{G}_o(\mathbf{r}_j,\mathbf{r}_k;\omega)+\mathbf{G}_h(\mathbf{r}_j,\mathbf{r}_k;\omega)$ for $j,k=1\ldots n$. Using matrix block multiplications, from Eq. (15) we get the following two relations in Eqs. (18) and (19). The first is the momentum conservation relation that has to be satisfied by self-fields E^e of point emitters as an optical theorem [25], and the second is the null-field condition for the polarizable bodies:

$$\frac{4\pi\omega^2}{c^2}[\bar{G}_o^{ee}\cdot P^e+\bar{G}_o^{eb}\cdot P^b]=E^e, \tag{18}$$

$$\frac{4\pi\omega^2}{c^2}[\bar{G}_o^{be}\cdot P^e+\bar{G}_o^{bb}\cdot P^b]=0. \tag{19}$$

Removing P^b in the above relations and substituting the result in Eq. (14), we get the global matrix with the modified Green dyads between pairs of emitters in the presence of the other polarizable bodies in this heterostructure:

$$\bar{G}^{ee}=\bar{G}_o^{ee}-\bar{G}_o^{eb}\cdot[\bar{G}_o^{bb}]^{-1}\cdot\bar{G}_o^{be}. \tag{20}$$

$\bar{G}^{ee}$ has ordered dyads $\mathbf{G}(\mathbf{r}_j,\mathbf{r}_k;\omega)=\mathbf{G}_o(\mathbf{r}_j,\mathbf{r}_k;\omega)+\mathbf{G}_h(\mathbf{r}_j,\mathbf{r}_k;\omega)$ for $j,k=1\ldots n$, and these are used instead of $\mathbf{G}_o(\mathbf{r}_j,\mathbf{r}_k;\omega)$ in Eq. (9) to assemble the self-energy matrices. Note that the diagonal entries of $\bar{G}^{ee}$ in Eq. (20) are nonzero, unlike its free-space correspondent $\bar{G}_o^{ee}$. These represent the additional self-interaction of the independent emitter due to other polarizable matter in proximity. But it is important to note why this method is significantly different from computing the modified Green dyads using a sum of all possible paths of interaction between two emitters in a heterostructure, which is the most obvious evaluation given all the Green dyads of free space or a homogeneous background. First, the total number of possible paths of interaction between two emitters

in an m body heterostructure is large, $C\binom{m}{l}$ for a subset of l bodies. Evaluation of the resulting vector and phase for each of these paths includes $(4\cdot 3^3\cdot l)$ multiplication operations—$(4\cdot 3^3)$ operations in the case of multiplying any two three-dimensional Green dyads in complex number arithmetic. Correspondingly, the number of arithmetic operations in evaluating the perturbations to free-space Green dyads is large, $\sim\Sigma_{l=1}^{m} 4\cdot 3^3\cdot l\cdot C(_l^m) > 2^m$, an idea useless for $m \gg 1$. On the other hand, an evaluation using Eq. (20) involves $4\cdot 3^3 m^3$ multiplication operations at most. For $m\sim 10^4$, repeating such evaluations is possible today even with a personal computing device. A physical interpretation of Eq. (21) is thus meaningful, and this perturbation to the global matrix containing free-space Green dyads can be rewritten as a minimization problem shown below. This results from interpreting the inverse of a matrix A as projector into a vector space (Krylov subspace) of a minimum monic [implies $c_o = 1$ in Eq. (21)] polynomial of matrix A, expanded in the powers of the matrix $\bar{G}_o^{bb}$ as below [26]:

$$\begin{aligned}\bar{G}_o^{eb}\cdot[\bar{G}_o^{bb}]^{-1}\cdot\bar{G}_o^{be} &= \min_{p_m\in P_m}\|\bar{G}_o^{eb}\cdot p_m(\bar{G}_o^{bb})\cdot\bar{G}_o^{be}\|\\ &= \min\|c_o\bar{G}_o^{eb}\cdot\bar{G}_o^{be} + c_1\bar{G}_o^{eb}\cdot(\bar{G}_o^{bb})\cdot\bar{G}_o^{be}\\ &\quad + c_2\bar{G}_o^{eb}\cdot(\bar{G}_o^{bb})^2\cdot\bar{G}_o^{be} + \cdots + c_m\bar{G}_o^{eb}\\ &\quad\cdot(\bar{G}_o^{bb})^m\cdot\bar{G}_o^{be}\|,\end{aligned}\tag{21}$$

where p_m represents a polynomial of degree m and the full set of such possible polynomials is P_m. Thus $p_m(\bar{G}_o^{bb})$ includes all powers of the global matrix of Green dyads coupling the bodies, and note that $(\bar{G}_o^{bb})^l$ contains the resulting dyads of all the possible l interaction paths between them. Even paths involving more than m interactions are implicitly included as they are anyway linear combinations of the above paths. Hence, Eq. (21) represents a minimum of sum over all paths of interaction between any pair of emitters, and this method is thus equivalent to a Lagrangian solution of the problem.

C. Radiative and Nonradiative Contributions to Self-Energy Components

The radiative and nonradiative parts of this collective emission have to be determined for a comparison with experimental measurements of the radiative properties and decay rates. The nonradiative losses of a collective mode of emission depend on the interactions of the emitters through the other bodies in addition to their internal nonradiative relaxations. The nonradiative absorption of an isolated body significantly smaller than wavelength is well approximated by $\Im[\bar{\alpha}(\mathbf{r}_j)\mathbf{E}^*(\mathbf{r}_j)\cdot\mathbf{E}(\mathbf{r}_j)]$ and depends only on the imaginary part of $\bar{\alpha}$ [27]. Here, the contributions of the imaginary parts of $\bar{\alpha}$ (of *all* the interacting polarizable bodies) to the self-energies of interaction between *any* two emitters have to be decomposed. In the m body system, these components contain both the real and imaginary parts of polarizability, as radiative interactions among bodies can precede a nonradiative loss. The radiative contributions of an isolated small body involve the real part and magnitude of its $\bar{\alpha}$, i.e., only the real part of its $\bar{\alpha}^{-1}$. Thus we have two components to the imaginary part of self-energy matrix Γ_{jk}, one that involves the imaginary part of $\bar{\alpha}^{-1}$ of a body as a factor in the self-energy components, and the exclusion that represents the radiative contributions from all interacting bodies. These are represented by the nonradiative decay matrix Γ_{jk}^{nr} and the radiative decay matrix Γ_{jk}^{r}, respectively. Evaluation of the radiative or nonradiative decay of collective eigenstates requires such a decomposition of self-energy matrix, as a function of the specific geometry defined by the global matrix of Green dyads. Using matrix decomposition identities for the inverse of sum of two full-rank matrices, we can derive these nonradiative and radiative parts of the total self-energy matrix as given below, where diagonal terms $-\delta_{jk}i\Gamma_o^r/2$ and $-\delta_{jk}i\Gamma_o^{nr}/2$ are included after integration over frequencies around ω_o. Let

$$\Sigma_{jk}^r = \Delta_{jk}^r - \frac{i\Gamma_{jk}^r}{2} = \frac{-2\pi q^2\omega}{mc^2}\mathbf{e}_j\cdot\mathbf{G}^r(\mathbf{r}_j,\mathbf{r}_k;\omega)\cdot\mathbf{e}_k - \delta_{jk}\frac{i\Gamma_o^r}{2},\tag{22}$$

$$\Sigma_{jk}^{nr} = \Delta_{jk}^{nr} - \frac{i\Gamma_{jk}^{nr}}{2} = \frac{-2\pi q^2\omega}{mc^2}\mathbf{e}_j\cdot\mathbf{G}^{nr}(\mathbf{r}_j,\mathbf{r}_k;\omega)\cdot\mathbf{e}_k - \delta_{jk}\frac{i\Gamma_o^{nr}}{2},\tag{23}$$

where the required Green dyads are

$$\begin{aligned}&\mathbf{G}^r(\mathbf{r}_j,\mathbf{r}_k;\omega) = \bar{G}^r(j,k)\quad\text{and}\\ &\mathbf{G}^{nr}(\mathbf{r}_j,\mathbf{r}_k;\omega) = \bar{G}^{nr}(j,k)\quad\text{for } j,k = 1\ldots n.\end{aligned}\tag{24}$$

The required radiative and nonradiative Green dyads and their corresponding global matrices in Eq. (24) can be derived using a decomposition of $\bar{G}_o^{bb}$ containing the imaginary and real part of polarizability as in Eqs. (25) and (26). Our objective here is to evaluate the corresponding contributions to $[\bar{G}_o^{bb}]^{-1}$ and the Green dyads coupling emitters, $\bar{G}^{ee}$ in Eq. (20). These result in the radiative and nonradiative global dyads of Eq. (24) evaluated by Eqs. (28) and (29). We decompose the global matrix of Green dyads coupling the polarizable bodies into

$$\bar{G}_o^{bb} = \bar{G}_o^{bb1} + \bar{G}_o^{bb2},\tag{25}$$

where

$$\begin{aligned}&\bar{G}_o^{bb1}(j,k) = \mathbf{G}_o(\mathbf{r}_{n+j},\mathbf{r}_{n+k};\omega) - \delta_{jk}\Re(\bar{\alpha}_{n+j}^{-1}(\omega)),\\ &\bar{G}_o^{bb2}(j,k) = -\delta_{jk}\Im(\bar{\alpha}_{n+j}^{-1}(\omega))\quad\text{for } j,k = 1\ldots m,\end{aligned}\tag{26}$$

when

$$(\bar{\mathrm{A}}+\bar{\mathrm{B}})^{-1} = \bar{\mathrm{A}}^{-1} - (\bar{\mathrm{I}}+\bar{\mathrm{A}}^{-1}\bar{\mathrm{B}})^{-1}\bar{\mathrm{A}}^{-1}\bar{\mathrm{B}}\bar{\mathrm{A}}^{-1},\tag{27}$$

$$\bar{G}^r = \bar{G}_o^{ee} - \bar{G}_o^{eb}\cdot[\bar{G}_o^{bb1}]^{-1}\cdot\bar{G}_o^{be},\tag{28}$$

$$\bar{G}^{nr} = \bar{G}_o^{eb}\cdot\{\bar{\mathrm{I}} + [\bar{G}_o^{bb1}]^{-1}\cdot\bar{G}_o^{bb2}\}^{-1}\cdot[\bar{G}_o^{bb1}]^{-1}\cdot\bar{G}_o^{bb2}\cdot[\bar{G}_o^{bb1}]^{-1}\cdot\bar{G}_o^{be}.\tag{29}$$

Γ_o^{nr}, the nonradiative relaxation of the independent emitter, can be explicitly introduced in the self-energy and nonradiative decay matrices, and we assume the quantum efficiency Q_o and radiative rate of an independent isolated emitter Γ_o^r are its only known properties other than $\hbar\omega_o$. Note that diagonal entries of the self-energy matrix in Eqs. (22) and (23) include the explicitly added decay rates of the independent emitter as its

imaginary parts, and in addition, the evaluated decay rates and the energy shifts due to the other bodies in proximity, i.e., the Purcell effect on independent emitters. When $\bar{G}_o^{bb2}$ is not a full-rank matrix because one or more of the m polarizable volumes have $\Im(\bar{\alpha}) = \bar{0}$, Eq. (27) can be replaced by other matrix decomposition identities. Similarly, note that $\bar{G}_o^{bb1}$ is invertible when all the real parts of polarizability of the bodies are nonzero and has the same requirement in such special cases otherwise. Formulae for inverting a sum of an invertible and a rank one matrix can be recursively used where matrix $\bar{\mathrm{B}}$ in $(\bar{\mathrm{A}} + \bar{\mathrm{B}})^{-1}$ need not be invertible and of low rank [28–30]. Similarly, matrix deflating techniques are also possible when the real or imaginary part of the polarizability of some of the bodies is zero, and these methods can be found elsewhere [31]. As explained in Section 2.A, the eigenstates J and their decay rates are given by the normalized eigenvectors and the eigenvalues of Σ, respectively, as in Eq. (30). The real parts of eigenvalues are the energy shifts Δ_J and its imaginary part is half the decay rate $\Gamma_J/2$. The radiative decay rate Γ_J^r is given by the vector–matrix–vector product $J^\dagger \Gamma^r J$ described by the state representation in Eq. (31):

$$\Sigma|J\rangle = \Delta_J - \frac{i\Gamma_J}{2}|J\rangle, \tag{30}$$

$$\Gamma_J^r = \langle J|\Gamma^r|J\rangle. \tag{31}$$

The normalized quantum efficiency Q_h and *power* of emitters P_h in the heterostructure are given by the sum over the corresponding values of eigenstates as below [10]:

$$Q_h = \frac{1}{n}\sum_J Q_J \quad \text{and} \quad P_h = \sum_J Q_J \Gamma_J^r, \tag{32}$$

where

$$Q_J = \frac{\Gamma_J^r}{\Gamma_J^r + \Gamma_o^{nr}}. \tag{33}$$

Note that in the above definitions of Q, which indicate efficiency of the emitters, we have not included the nonradiative decay of a part of this emission in the metal particles. An alternative definition that includes this absorption loss in the metal particles should have Γ_J, the total decay rate of the eigenstate J as the denominator in Eq. (33). The total rate of decay from an ensemble of heterostructures as observed by lifetime measurements can be traced using the energy radiated by all eigenstates. In determining the power and tracing the decay as in Eqs. (33) and (34) note that we do not evaluate the decay of a specific initial state in a particular geometry of heterostructure. That requires expanding the prepared initial state using a weighted sum of the eigenstates, and this is not of relevance in experiments where initial states of the system are unknown and random (due to the nonradiative process that it accompanies). Alternately, we can determine the eigenstates for all possible random permutations in a heterostructure along with random orientations of its dipole emitters. Once the collective eigenstates of a particular geometry are determined, we sum the emitted power and the decay of all its eigenstates. These quantities represent an average of these observables over the full phase space of possible initial states in the geometry, which are further averaged over random geometries. These results can be directly compared to experimental measurements involving a large ensemble of such structures:

$$I(t) = \sum_J Q_J e^{-\Gamma_J t}. \tag{34}$$

Before we present numerical results of this evaluation, we conclude this section with a note on few limiting cases and the corrections required. The limits of the dyadics of point dipoles used and the effects of discretization of a body have to be discussed. This method is general enough to include arbitrary, local volume discretization of a body in *multiple* scales for problems with any special cases. One such case is when two small bodies are closely spaced and a finer discretization of the body is required to include multi-pole interactions, for example, when distance between centers $\to 2a$, where a is radius of a spherical particle. To include l pole effects sufficiently, a finer discretization of a body in dipolar representation scales the global matrices by l^3 in general, and thus computation by $(l^3)^3 = l^9$. Explicit use of higher-order Mie modes of a sphere, its l pole polarizability α_l, and its Green dyads in the discretized representation of geometry to be evaluated is also possible for large spherical sub-volumes. For if more Green dyads of modes up to l for any polarizable volume are explicitly included in the global matrix in Eq. (15), the matrix dimensions increase by a factor of only l and this will result in an increase in computation by a factor of only l^3. Also, one should expect that when the distance between the surface of a body and an emitter is on the order of charge separations $d = p/q$, an evaluation using the dyads of point dipoles in Eq. (13) may be not accurate. At these small separations $\sim$1 nm, charge screening in the body may not be complete, local inhomogeneity of $\bar{\varepsilon}$ may not be negligible, and electron-hole pairs can be created. Such energy transfer mechanisms can result in coupling on the order of $\sim r^4$ and higher, which may not be represented sufficiently by finer discretization of the body alone. However, studies show that these local deviations are significantly suppressed by both nonlinear effects and quantization, resulting in a freezing of higher-order classical modes [32]. These effects can result in a domination of the radiative terms on the interaction with the polarizable matter even at these close separations [33,34]. Nevertheless, corrections to $\mathbf{G}_o(\mathbf{r}_j, \mathbf{r}_k; \omega)$ for these mechanisms of interaction may be included for emitter-body separations less than 1 nm in any special cases. Modifications required to $\mathbf{G}_o(\mathbf{r}_j, \mathbf{r}_k; \omega)$, in case of a strongly interacting surface in the near-field of the heterostructure, are presented in Appendix B.

3. EXAMPLES AND NUMERICAL RESULTS

This section presents numerical results to highlight the significance of collective emission characteristics possible when multiple emitters interact with multiple bodies. Numerical evaluations of collective eigenstates of emission from emitter-metal nanoparticle ensembles were performed. We compare the results of the method presented here (named NS) with two other evaluations of the same structures: (1) independent emitters interacting with multiple metal particles (named IE for independent emitters) and (2) a set of emitters

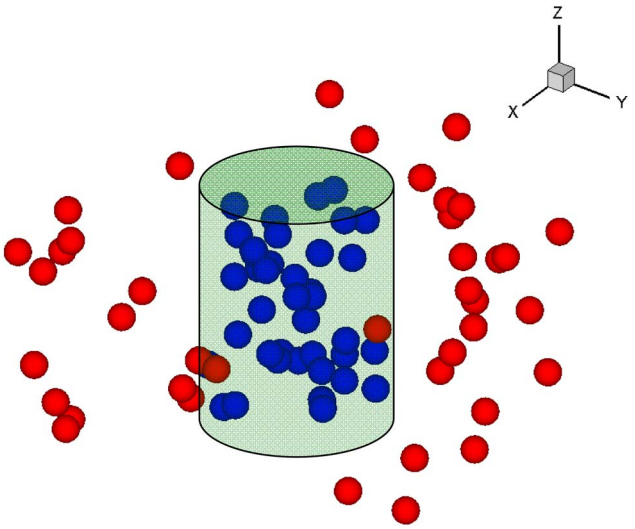

Fig. 1. Sketch of the heterostructure (not to scale). In G1 blue spheres represent the dipole emitters and the red spheres represent metal particles, and vice versa in G2.

collectively interacting with many independent metal particles where interaction among metal particles is ignored (named EPS, for extended Pustovit–Shahbazyan model explained in Appendix A). The objective is to highlight that while the differences with the former show the significance of collective modes of emission in such heterostructures, the differences with the latter emphasize that the collective modes of emitters are sensitive to an increase in local density of optical states (LDOS) due to interactions among many metal particles. Moreover, these results are shown to be approximated by (1) a case where coupling among the emitters is weak relative to the available LDOS and (2) a case of interaction of the collection of emitters with one or a few metal particles.

Consider a structure where the emitters are randomly distributed inside a cylinder of radius 20 nm and height 40 nm, while the metal particles are all randomly distributed outside this cylinder; see Fig. 1. The position vectors $\mathbf{r}_p$ of the metal particles represent a random normal distribution in $\Re^2$ with a mean distance of 35 nm from the axis of the cylinder (and a standard deviation of 4 nm). The distribution of these particles

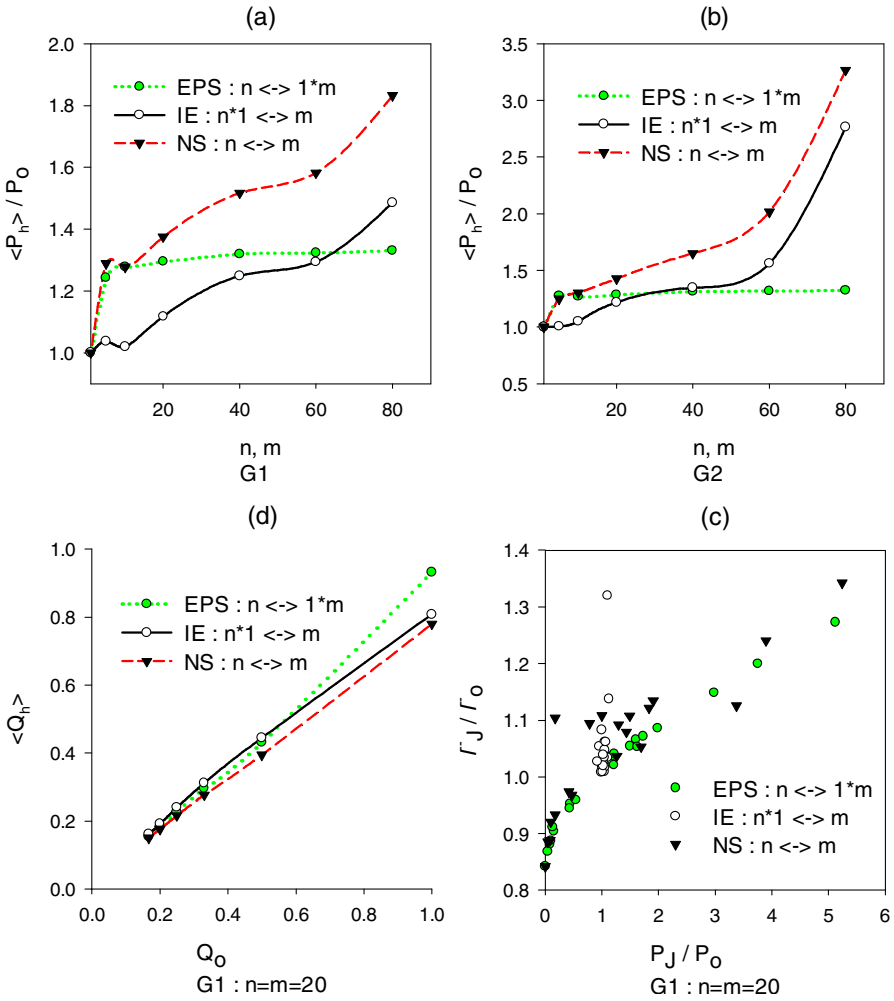

Fig. 2. (a) Ensemble averages of power enhancement in G1. (b) Ensemble averages of power enhancement in G2. (c) Eigenstates of decay rates and emitted power for one example case in the ensemble of 150 evaluations. J represents individual emitters in the case of IE evaluation, and the eigenstates in the other two evaluations, and (d) ensemble averages of the normalized quantum efficiency of heterostructures as a function of quantum efficiency Q_o of isolated emitters for $n = m = 20$ in G1.

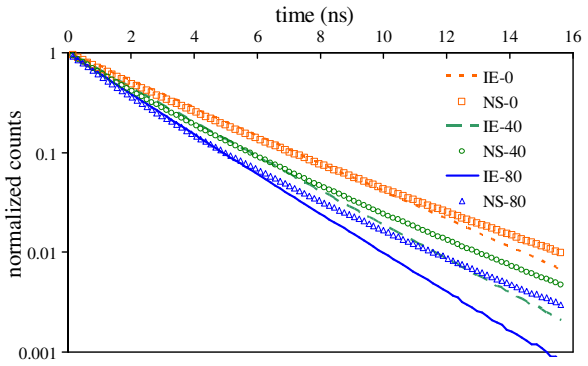

Fig. 3. Normalized time traces of decay representing 40 dipole emitters with varying numbers (0, 40, 80) of 3 nm radii gold particles in a G1 heterostructure ensemble: $\hbar\omega_o = 2.21$ eV, $Q_o = 0.5$, and $\Gamma_o^r = 1/2 \times 10^9$ rad/s for the isolated emitters in the film.

in z direction (parallel to the axis of the cylinder) is a random uniform distribution in $\Re^1$. $\mathbf{e}_j$ are unit vectors of a random uniform distribution in $\Re^3$ representing the emitter polarizations. The position vectors $\mathbf{r}_e$ of the emitters represent a different random uniform distribution in $\Re^3$ throughout the interior space of the cylinder. Such ordered self-assembled films consisting of quantum dots and metal particles are in fact studied experimentally [7]. This geometry is named G1, and an inversion of such distributions where the emitters are outside the cylinder while metal particles are inside is named G2.

Using the computed collective eigenstates, the results presented include the power enhancements evaluated, relative decay rates, quantum efficiencies, and time traces of decay using Eqs. (30)–(34). The results produced here involve gold spheres 3 nm in radii and dipole emitters with $\hbar\omega_o = 2.21$ eV (that corresponds to a free-space wavelength of ~560 nm). We also assume that this heterostructure is embedded in a medium with relative permittivity $\varepsilon/\varepsilon_0 = 2.25$ to represent realistic polymeric materials. Isolated emitters are assumed to have quantum efficiency of 1/6; and as shown later Q_o has an almost linear effect on the quantum efficiency of the heterostructure and there is no loss of generality. The power of emission, due to a continuous excitation, and the lifetimes are the typically measured variables in an experimental study of characteristics of emission. Figure 2(a) shows the power enhancement in the G1 heterostructure relative to an equal number of isolated emitters; there are two clear regimes apparent in this plot. These results are ensemble averages over 150 random permutations of the emitters and metal particles.

First, in the limit of a few metal particles ($m \leq 10$), the full evaluation (NS) matches with the EPS evaluation of m independent metal particles interacting with the collection

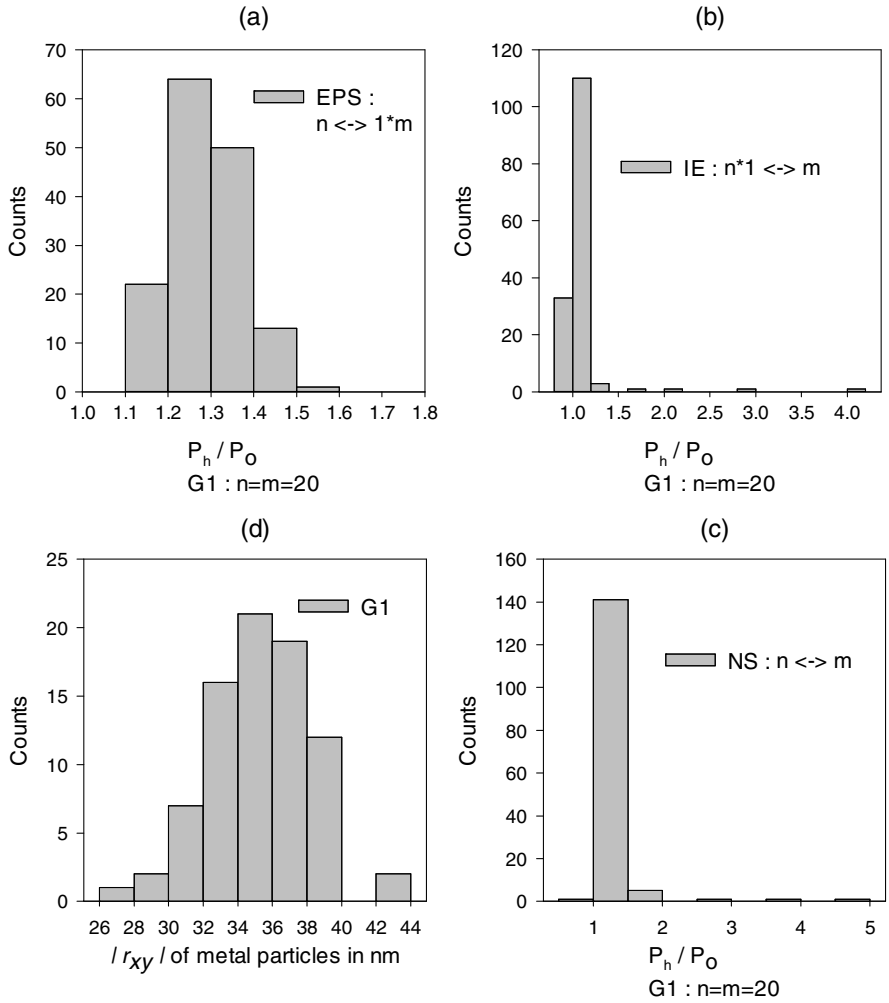

Fig. 4. Ensemble values of power enhancement in G1 for $m = n = 20$. (a) EPS, independent metal particles; (b) IE, independent emitters; and (c) NS, interacting emitters and metal particles. (d) Example distribution of 80 metal particles in the XY plane of G1.

of emitters. Here the collective interaction among emitters results in a significant increase in the power enhancement, and this is not revealed in the independent emitter (IE) characteristics. As the number of particles increases further ($m \geq 60$), strong interactions among metal particles can result in a large increase in LDOS, which breaks the accuracy of the EPS evaluation. This regime is dominated by the LDOS available to the emitter, and the interactions between emitters seem to play a weaker role compared to the interactions between the metal particles.

In the inverted complementary structure G2, the interaction between the emitters that are spread outside the cylinder is expected to be weaker. But the interaction among the metal particles is more significant here and the increase of LDOS has a larger effect on the power of emission. Thus the collective excitation regime of the emitters seems to have a smaller parametric range and is of lesser significance than in G1 as shown in Fig. 2(b). However, one should be cautioned that power enhancement is not a sufficient indicator of the underlying emission process. The lifetimes measured in such heterostructures are governed by the collective eigenstates, as shown in the example shown in Fig. 2(c). The above results in Figs. 2(a)–2(c) were all evaluated for isolated emitters having a quantum efficiency of 1/6. However, Fig. 2(d) shows that a change in the quantum efficiency of isolated emitters does not change the conclusions above. Ensemble averages of $m = n = 20$ in G1 are evaluated over a range in Q_o to show its almost linear effect on the normalized quantum efficiency of the heterostructure Q_h in Eq. (32). The apparent lifetimes measured in such heterostructures can be significantly dominated by the slower eigenstates of the collective excitation and show notable differences with an isolated emitter interacting with the metal particles. Figure 3 shows emission dynamics for a few cases that use the calculated eigenstates and Eq. (34) to trace the decay of the collective excitations. Emitters of even moderate quantum efficiency ($Q_o = 0.5$) show a clear shift in the decay curves of their collective emission. Their apparent decay seems to become slower with time, which is an effect of multiple eigenstates.

In all the above calculations, raw data of the ensemble show approximate normal distributions confirming that the mean values represent the general behavior of a heterostructure (G1 or G2) for a specific case of m, n. The raw data of one such ensemble are shown in Fig. 4. As expected, IE and NS evaluations have marginally larger standard deviations in the ensembles due to their higher sensitivity to the permutation of metal-particle locations. We have limited ourselves to results that highlight that collective emission can be notably different from independent emission. The full exploitation of the method presented here may need other numerical studies on a larger parametric space on many other heterostructures. These studies may help us to control exciton–plasmon couplings and resulting emission using low concentrations of even smaller metal particles, a regime that can certainly be very different from such effects on independent emitters.

4. CONCLUSION

A method to evaluate characteristics of eigenstates of an interacting set of n dipole emitters and other polarizable matter of generalized geometries was presented. The role of self-energy matrices in the estimation of their collective eigenstates was described, and the required relations for decomposition of their radiative and nonradiative parts were also derived. Closed form relations to evaluate Green tensors using the global matrices of Green dyads coupling entity pairs in free-space (or a homogeneous background medium) were produced. These relations were also shown to satisfy general laws of physics such as a Lagrangian solution of the problem and the optical theorem for many point emitters and other polarizable bodies interacting among themselves. The possible modifications for special limiting cases were discussed and an extension of this method to evaluate the collective interactions with a surface is presented in Appendix B. Moreover, the significant effects of n coupled emitters interacting with m polarizable bodies were highlighted using numerical results. The heterostructures used in these numerical examples provided a concise view of the rich behavior of emission possible in collective systems. This method of enumerating eigenstates of emission and radiative properties in strongly interacting emitter matter systems provides a new path to deeper understanding of optical metamaterials.

APPENDIX A: PUSTOVIT–SHAHBAZYAN MODEL FOR *m* INDEPENDENT METAL PARTICLES

The self-energy matrix of an ensemble of dipole emitters interacting with a single spherical metal particle was described by Pustovit and Shahbazyan, and an analytical solution of the green tensors was derived under long-wavelength approximation [10]. There, the phase of the oscillators was fixed while the amplitudes were modified due to the common field, as described by the self-energy matrix of the ensemble:

$$\Sigma_{jk}(\omega) = \frac{-2\pi q^2 \omega_o}{mc^2}\mathbf{e}_j \cdot \mathbf{G}(\mathbf{r}_j, \mathbf{r}_k; \omega) \cdot \mathbf{e}_k,$$
$$\text{where } \Gamma_o^r = \frac{2\ kq^2\omega_o}{3\ mc^2} \quad \text{and} \quad \omega \approx \omega_o. \tag{A1}$$

The modified Green dyads coupling the dipole emitters $P_j\mathbf{e}_j$ in the presence of a single spherical metal particle centered at $\mathbf{r}_p$ were derived. They satisfy the following relations where $\varepsilon_p, \varepsilon_o$ and θ are the permittivity of metal, free space and the step-function relating them, for a spherical particle of radius R:

$$\frac{4\pi\omega^2}{c^2}\sum_k \mathbf{G}_p(\mathbf{r}, \mathbf{r}_k; \omega) \cdot \mathbf{e}_k p_k e^{i\phi_k} = \mathbf{E}(\mathbf{r}, \omega),$$

where

$$k^2\varepsilon(\mathbf{r}) \cdot \mathbf{G}_p(\mathbf{r}, \mathbf{r}_j; \omega) - \nabla \times \nabla \times \mathbf{G}_p(\mathbf{r}, \mathbf{r}_j; \omega) = \delta(\mathbf{r} - \mathbf{r}_j),$$
$$\text{and } \varepsilon(\mathbf{r}) = \varepsilon_p\theta(R - \|\mathbf{r} - \mathbf{r}_p\|) + \varepsilon_0\theta(\|\mathbf{r} - \mathbf{r}_p\| - R). \tag{A2}$$

The Green dyadic between the dipole emitters at $\mathbf{r}_j, \mathbf{r}_k$, due to all the metal particles not interacting among each other, can then be derived by a sum of these modified Green dyads in the presence of all the single metal particles at the locations $\mathbf{r}_p$.

$$\mathbf{G}(\mathbf{r}_j, \mathbf{r}_k; \omega) = \mathbf{G}_o(\mathbf{r}_j, \mathbf{r}_k; \omega) + \sum_p \mathbf{G}_p(\mathbf{r}_j, \mathbf{r}_k; \omega), \tag{A3}$$

and

$$\Sigma_{jk} = \frac{3\Gamma_o^r}{4\,k^3}\left\{\frac{\mathbf{e}_j\cdot\mathbf{e}_k}{r_{jk}^3} - \frac{3(\mathbf{e}_j\cdot\mathbf{r}_{jk})(\mathbf{e}_k\cdot\mathbf{r}_{jk})}{r_{jk}^5} - \sum_l \alpha_l T_{jk}^l\right\} - \frac{i\Gamma_o^r}{2}\{\mathbf{e}_j\cdot\mathbf{e}_k - \alpha_1 K_{jk}^1 + |\alpha_1|^2 T_{jk}^1\} - \delta_{jk}\frac{i\Gamma_o^{nr}}{2}, \quad \text{(A4)}$$

where

$$T_{jk}^l = \sum_p \frac{4\pi}{2l+1}\sum_{-l}^{+l}[\mathbf{e}_j\cdot\psi_{lm}(\mathbf{r}_j-\mathbf{r}_p)][\mathbf{e}_k\cdot\psi_{lm}(\mathbf{r}_k-\mathbf{r}_p)], \quad \text{and}$$

$$K_{jk}^l = \sum_p \frac{4\pi}{2l+1}\sum_{-l}^{+l}[\mathbf{e}_j\cdot\psi_{lm}(\mathbf{r}_j-\mathbf{r}_p)][\mathbf{e}_k\cdot\chi_{lm}(\mathbf{r}_k-\mathbf{r}_p)],$$

$$\psi_{lm}(\mathbf{r}) = \nabla\left[\frac{Y_{lm}(\mathbf{r})}{r^{l+1}}\right], \qquad \chi_{lm}(\mathbf{r}) = \nabla[r^l Y_{lm}(\mathbf{r})]. \quad \text{(A5)}$$

$Y_{lm}(\mathbf{r})$ are the spherical harmonics and specifically, the dipole mode components are given by

$$K_{jk}^1 = \sum_p \frac{1}{\|\mathbf{r}_j-\mathbf{r}_p\|^3}\left\{\mathbf{e}_j\cdot\mathbf{e}_k - \frac{3(\mathbf{e}_j\cdot(\mathbf{r}_j-\mathbf{r}_p))(\mathbf{e}_k\cdot(\mathbf{r}_j-\mathbf{r}_p))}{\|\mathbf{r}_j-\mathbf{r}_p\|^2}\right\},$$

$$T_{jk}^1 = \sum_p \frac{1}{\|\mathbf{r}_k-\mathbf{r}_p\|^3\|\mathbf{r}_j-\mathbf{r}_p\|^3} \times\left\{\mathbf{e}_j\cdot\mathbf{e}_k - \cdots\frac{3(\mathbf{e}_j\cdot(\mathbf{r}_j-\mathbf{r}_p))(\mathbf{e}_k\cdot(\mathbf{r}_j-\mathbf{r}_p))}{\|\mathbf{r}_j-\mathbf{r}_p\|^2} - \frac{3(\mathbf{e}_j\cdot(\mathbf{r}_k-\mathbf{r}_p))(\mathbf{e}_k\cdot(\mathbf{r}_k-\mathbf{r}_p))}{\|\mathbf{r}_k-\mathbf{r}_p\|^2} + \cdots \frac{9(\mathbf{e}_k\cdot(\mathbf{r}_k-\mathbf{r}_p))(\mathbf{e}_j\cdot(\mathbf{r}_j-\mathbf{r}_p))((\mathbf{r}_k-\mathbf{r}_p)\cdot(\mathbf{r}_j-\mathbf{r}_p))}{\|\mathbf{r}_j-\mathbf{r}_p\|^2\|\mathbf{r}_k-\mathbf{r}_p\|^2}\right\}. \quad \text{(A6)}$$

The self-energy matrix of the ensemble of emitters can be decomposed into its radiative and nonradiative decay parts as

$$\Gamma_{jk}^r = \Gamma_o^r\{\mathbf{e}_j\cdot\mathbf{e}_k - \alpha_1' K_{jk}^1 + |\alpha_1|^2 T_{jk}^1\} \quad \text{and}$$

$$\Gamma_{jk}^{nr} = \frac{3\Gamma_o^r}{2\,k^3}\sum_l \alpha_l'' T_{jk}^l - \delta_{jk}\frac{i\Gamma_o^{nr}}{2}, \quad \text{(A7)}$$

where $\alpha_l = \alpha_l' + i\alpha_l''$.

The l-pole polarizability of the spherical metal particle is given by

$$\alpha_l(\omega) = a^{2l+1}\left[\frac{\varepsilon(\omega,\mathbf{r}_p)-\varepsilon}{\varepsilon(\omega,\mathbf{r}_p)+(1+1/l)\varepsilon}\right], \quad \text{(A8)}$$

where a is radius of particle at $\mathbf{r}_p$.

APPENDIX B: NOTE ON SURFACE INTERACTIONS

The interaction of emitters and other bodies with a substrate/surface has been difficult to study because separable coordinates for analytical solutions do not exist, and Fresnel coefficients for near-field radiating sources do not have closed form relations that are easily computable [35–38]. An expansion of the fields in Cartesian coordinates with the surface represented by a coordinate plane is the more intuitive approach, though it involves integration over two dimensions [11]. Analytical forms of these solutions using additional series expansions were also provided recently [39]. A more convenient approach is to numerically calculate the components of a radiating dipole in the near field of the surface using the Sommerfeld identity for a spherical wave in free space as in Eq. (A9):

$$\frac{e^{ikr}}{4\pi r} = \frac{1}{4\pi}\int_0^\infty \frac{k_\rho}{k_z}J_o(\rho k_\rho)\exp(-ik_z|z|)\mathrm{d}k_\rho. \quad \text{(A9)}$$

The field from a radiating dipole over a surface can also be decomposed into cylindrical components parallel to the surface (ρ axis) and a plane wave perpendicular to the surface (z axis), similarly. Here, Sommerfeld relations with reflection coefficients for the perpendicular plane waves interacting with the surface are numerically converged to as in Eq. (A10). This requires the reflection coefficients R as a quadratic function of k_ρ [40,41]. For any two dipoles k and j at any distance z from the surface, and ρ from each other along the surface, the integral in Eq. (A10) has to converge over the complex domain of wave vector magnitudes k_ρ and involves appropriate branch cuts. The reflected component of the electric field due to a radiating dipole in the near field of a surface can then be represented as in Eq. (A11) [41,42]:

$$\frac{e^{ikr}}{4\pi r} = \frac{1}{4\pi}\int_0^\infty J_o(\rho k_\rho)\cdot R(k_\rho)\cdot\exp(-ik_z|z|)\mathrm{d}k_\rho, \quad \text{(A10)}$$

$$\mathbf{E}_{\text{surface},j} = \sum_{k=1}^{N}\left[\bar{S}_{jk} + \frac{k_s^2(k_o^2-k_s^2)}{\varepsilon_0(k_o^2+k_s^2)}\mathbf{G}_o^I(\mathbf{r}_j,\mathbf{r}_k;\omega)\right]\cdot\mathbf{P}_k, \quad \text{(A11)}$$

where $\bar{S}_{jk}$ is a 3×3 matrix containing Sommerfeld integral terms of the field for dipoles k and j, and k_o and k_s are the wave numbers in free-space/homogeneous background and the surface, respectively. We do not proceed further into the aspects of numerical calculation of $\bar{S}_{jk}$ in this paper, and these methods are described in the above mentioned works. For a surface at $z=0$, with its normal in the z direction, the image dyadic Green's function matrix is defined as

$$\mathbf{G}_o^I(\mathbf{r}_j,\mathbf{r}_k;\omega) = -\mathbf{G}_o(\mathbf{r}_j,\mathbf{r}_k;\omega)\cdot\mathbf{I}_R, \quad \text{(A12)}$$

where $\mathbf{I}_R$ is the reflection dyad $\mathbf{I}_R = \mathbf{e}_x\mathbf{e}_x + \mathbf{e}_y\mathbf{e}_y - \mathbf{e}_z\mathbf{e}_z$.

The *surface-modified* Green dyads of the background medium $\mathbf{G}_o^s(\mathbf{r}_j,\mathbf{r}_k;\omega)$ can be introduced into Eq. (6) in place of $\mathbf{G}_o(\mathbf{r}_j,\mathbf{r}_k;\omega)$ for computing the self-energy matrices of a heterostructure on a surface, and they are

$$\mathbf{G}_o^s(\mathbf{r}_j,\mathbf{r}_k;\omega) = \bar{S}_{jk} + \mathbf{G}_o(\mathbf{r}_j,\mathbf{r}_k;\omega)\cdot\left(\mathbf{I} - \frac{k_s^2(k_o^2-k_s^2)}{\varepsilon_0(k_o^2+k_s^2)}\mathbf{I}_R\right). \quad \text{(A13)}$$

ACKNOWLEDGMENTS

I am grateful to Bobby Philip, Oak Ridge National Laboratory, for many fruitful discussions and his comments on the manuscript.

REFERENCES

1. M. R. Philpott, "Effect of surface plasmons on transitions in molecules," J. Chem. Phys. **62**, 1812–1817 (1975).
2. D. Kleppner, "Inhibited spontaneous emission," Phys. Rev. Lett. **47**, 233–236 (1981).
3. H. Kuhn, "Classical aspects of energy transfer in molecular systems," J. Chem. Phys. **53**, 101–108 (1970).
4. D. Ratchford, F. Shafiei, S. Kim, S. K. Gray, and X. Li, "Manipulating coupling between a single semiconductor quantum dot and single gold nanoparticle," Nano Lett. **11**, 1049–1054 (2011).
5. J. S. Biteen, N. S. Lewis, H. A. Atwater, H. Mertens, and A. Polman, "Spectral tuning of plasmon-enhanced silicon quantum dot luminescence," Appl. Phys. Lett. **88**, 131109 (2006).
6. J. S. Biteen, L. A. Sweatlock, H. Mertens, N. S. Lewis, A. Polman, and H. A. Atwater, "Plasmon-enhanced photoluminescence of silicon quantum dots: simulation and experiment," J. Phys. Chem. C **111**, 13372–13377 (2007).
7. M. Haridas and J. K. Basu, "Controlled photoluminescence from self-assembled semiconductor-metal quantum dot hybrid array films," Nanotechnology **21**, 415202 (2010).
8. A. O. Govorov, G. W. Bryant, W. Zhang, T. Skeini, J. Lee, N. A. Kotov, J. M. Slocik, and R. R. Naik, "Exciton-plasmon interaction and hybrid excitons in semiconductor-metal nanoparticle assemblies," Nano Lett. **6**, 984–994 (2006).
9. V. N. Pustovit and T. V. Shahbazyan, "Cooperative emission of light by an ensemble of dipoles near a metal nanoparticle: the plasmonic Dicke effect," Phys. Rev. Lett. **102**, 077401 (2009).
10. V. N. Pustovit and T. V. Shahbazyan, "Plasmon-mediated superradiance near metal nanostructures," Phys. Rev. B **82**, 075429 (2010).
11. L. Novotny and B. Hecht, *Principles of Nano-Optics* (Cambridge, 2006).
12. M. L. Andersen, S. Stobbe, A. S. Sørensen, and P. Lodahl, "Strongly modified plasmon–matter interaction with mesoscopic quantum emitters," Nat. Phys. **7**, 215–218 (2011).
13. A. Thrańhardt, C. Ell, G. Khitrova, and H. M. Gibbs, "Relation between dipole moment and radiative lifetime in interface fluctuation quantum dots," Phys. Rev. B **65**, 035327 (2002).
14. A. O. Barut and J. P. Dowling, "Quantum electrodynamics based on self-energy: Spontaneous emission in cavities," Phys. Rev. A **36**, 649–654 (1987).
15. M. Brune, F. Schmidt-Kaler, A. Maali, J. Dreyer, E. Hagley, J. M. Raimond, and S. Haroche, "Quantum Rabi oscillation: a direct test of field quantization in a cavity," Phys. Rev. Lett. **76**, 1800–1803 (1996).
16. H. T. Dung, L. Knöll, and D. G. Welsch, "Decay of an excited atom near an absorbing microsphere," Phys. Rev. A **64**, 013804 (2001).
17. C. Van Vlack, P. T. Kristensen, and S. Hughes, "Spontaneous emission spectra and quantum light-matter interactions from a strongly coupled quantum dot metal-nanoparticle system," Phys. Rev. B **85**, 075303 (2012).
18. R. H. Dicke, "Coherence in spontaneous radiation processes," Phys. Rev. **93**, 99–110 (1954).
19. N. Skribanowitz, I. P. Herman, J. C. MacGillivray, and M. S. Feld, "Observation of Dicke superradiance in optically pumped HF gas," Phys. Rev. Lett. **30**, 309–312 (1973).
20. D. Pavolini, A. Crubellier, P. Pillet, L. Cabaret, and S. Liberman, "Experimental—evidence for subradiance," Phys. Rev. Lett. **54**, 1917–1920 (1985).
21. R. G. DeVoe and R. G. Brewer, "Observation of superradiant and subradiant spontaneous emission of two trapped ions," Phys. Rev. Lett. **76**, 2049–2052 (1996).
22. I. S. Nikolaev, W. Vos, and A. Koenderink, "Accurate calculation of the local density of optical states in inverse-opal photonic crystals," J. Opt. Soc. Am. B **26**, 987–997 (2009).
23. A. A. Svidzinsky, J. Chang, and M. O. Scully, "Cooperative spontaneous emission of atoms: Many-body eigenstates, the effect of virtual Lamb shift processes, and analogy with radiation of classical oscillators," Phys. Rev. A **81**, 053821 (2010).
24. B. T. Draine and J. Goodman, "Beyond Clausius-Mossotti—Wave propagation on a polarizable point lattice and the discrete dipole approximation," Astrophys. J. **405**, 685–697 (1993).
25. M. Venkatapathi, "Emitter near an arbitrary body: Purcell effect, optical theorem and the Wheeler-Feynman absorber," J. Quant. Spectrosc. Radiat. Transfer **113**, 1705–1711 (2012).
26. L. N. Trefethen and D. Bau, *Numerical Linear Algebra* (SIAM, 1997).
27. C. F. Bohren and D. F. Huffman, *Absorption and Scattering of Light by Small Particles* (Wiley, 1983), p. 136.
28. H. V. Henderson and S. R. Searle, "On deriving the inverse of a sum of matrices," SIAM Rev. **23**, 53–60 (1981).
29. K. S. Miller, "On the inverse of the sum of matrices," Math. Mag. **54**, 67–72 (1981).
30. D. J. Tylavsky and G. R. L. Sohle, "Generalization of the matrix inversion lemma," Proc. IEEE **74**, 1050–1052 (1986).
31. J. Demmel, *Applied Numerical Linear Algebra* (SIAM, 1996).
32. D. C. Marinica, A. K. Kazansky, P. Nordlander, J. Aizpurua, and A. G. Borisov, "Quantum plasmonics: nonlinear effects in the field enhancement of a plasmonic nanoparticle dimer," Nano Lett. **12**, 1333–1339 (2012).
33. V. N. Pustovit and T. V. Shahbazyan, "Fluorescence quenching near small metal nanoparticles," J. Chem. Phys. **136**, 204701 (2012).
34. V. N. Pustovit and T. V. Shahbazyan, "Resonance energy transfer near metal nanostructures mediated by surface plasmons," Phys. Rev. B **83**, 085427 (2011).
35. A. Sommerfeld, "Propagation of waves in wireless telegraphy," Ann. Phys. Leipz. **28**, 665–736 (1909).
36. A. Sommerfield, "Propagation of waves in wireless telegraphy," Ann. Phys. Leipz. **81**, 1135–1153 (1926).
37. A. Sommerfield, *Partial Differential Equations of Physics* (Academic, 1949).
38. A. Baňos, *Dipole Radiation in the Presence of a Conducting Half-Space* (Pergamon, 1966).
39. G. Y. Panasyuk, J. C. Schotland, and V. A. Markel, "Short-distance expansion for the electromagnetic half-space Green's tensor: general results and an application to radiative lifetime computations," J. Phys. A Math. Theor. **42**, 275203 (2009).
40. D. L. Lager and R. J. Lytle, "Fortran subroutines for the numerical evaluation of Sommerfeld integrals unter anterem," Lawrence Livermore Laboratory Report UCRL-51821 (1975).
41. A. Mohsen, "On the evaluation of Sommerfeld integrals," IEE Proc. Part H **129**, 177–182 (1982).
42. R. Schmehl, B. M. Nebeker, and E. D. Hirleman, "Discrete-dipole approximation for scattering by features on surfaces by means of a two-dimensional fast Fourier transform technique," J. Opt. Soc. Am. A **14**, 3026–3036 (1997).